Analysis and Simulation of Multipath Interference of FM Subcarrier Digital Signals

Linda Zeger*, Pei Chen, and Hisashi Kobayashi
Department of Electrical Engineering
Princeton University
Princeton, New Jersey 08544, USA
Fax: (609) 258-3745; E-mail: hisashi@ee.princeton.edu

Abstract

We present analytical results characterizing the effects of multipath interference on an FM subcarrier data channel. A closed form expression for the FM discriminator output (or the instantaneous received frequency) is obtained when there are M reflected path signals in addition to the primary path signal. We derive the power spectral density when the multipath interference is weak, and determine the conditions under which multipath interference causes nonlinearities in the instantaneous frequency of the received signal. In order to verify our analytical results, we have built an SPW simulator of HSDS (the high speed data service) system, and we have observed close agreement between our analysis and simulations.

The analytical techniques presented here could potentially be applied to other FM subcarrier systems, as well as to digital wireless systems that adopt FSK or its variants. Hence, our results could be useful in understanding noncoherent reception of the GSM digital cellular system, for example.

1 Introduction

Until recently, radio and television have been the only means for electronically disseminating information to a large number of people. However, demands for *datacasting* or *data broadcasting* are growing, and such technologies are being developed and introduced. An example of a successful market introduction of datacasting service is *teletext,* which uses subcarrier modulation of television broadcast signals. Another service actively pursued in the U.S., Europe, and Japan is data service using FM subcarrier multiplexing.

The baseband of an FM radio channel is approximately 100 kHz. The stereo audio signal is accommodated in the range of 0 to 53 kHz; the remaining baseband (i.e., 53 to 100 kHz) can be allocated to other information carrying spectra, which we call FM subcarriers. In Europe, an FM subcarrier service called RDS (radio data system) [3] is now in use. It provides an important feature to FM listeners in Europe, where the same program is often broadcast simultaneously by different FM stations. RDS allows a person in an automobile to continue listening to the same program without manually searching for the frequency when he or she moves into the coverage of a different FM station. The RDS spectrum uses 57 kHz as its subcarrier. A modified scheme, RBDS, was defined for U.S. markets and has been standardized. However, the services provided by RDS/RBDS have low speed, on the order of 1.2 Kbps.

Data services that offer a much higher speed and greater bandwidth efficient transmission than RDS or RDBS have recently been introduced: Seiko Communications' HSDS (high speed subcarrier data system) [1] and NHK's DARC (data radio channel) [2] are such examples, and they have recently begun to offer datacasting services in U.S./Europe, and Japan, respectively.

The performance of such FM subcarrier systems is primarily limited by multipath interference, as is the case with other digital wireless communication systems. Analysis of the multipath interference is rather complicated because the main carrier modulation is nonlinear (i.e., FM), and multipath effects introduce not only interference among data signals, but also, and more importantly, interference of the audio signal with the data signal.

In this paper we present our analysis and results of simulation experiments of multipath interference. An earlier version of some of the present work was recently presented [6]. We believe that our approach will also be useful to non-coherent reception of GSM and DECT, which adopt GMSK modulation, a form of FSK modulation.

*Currently with Lucent Technologies

2 FM Modulation with a Data Subcarrier

As described above, audio signals occupy the portion of the baseband spectrum from 0 to 53 kHz, while frequencies from 53 to 100kHz are normally unutilized. This upper portion of the spectrum can be used to transmit digital data, so that both the audio signal $A(t)$ and the data signal $D(t)$ modulate the FM carrier of frequency f_c. The instantaneous frequency of the transmitted signal is then

$$\omega(t) = 2\pi f_c + 2\pi f_d\,[\mathrm{A}(t) + \mathrm{D}(t)] = 2\pi f_c + 2\pi f_d S(t), \quad (1)$$

where f_d is the frequency deviation constant, and $S(t)$ is the total modulating signal. The transmitted signal is then given by

$$X(t) = A\cos(\int_0^t \omega(u)du). \quad (2)$$

We normalize the modulating signal amplitude so that

$$\max \mid S(t) \mid = 1. \quad (3)$$

The maximum swing is then the frequency deviation constant $\omega_d = 2\pi f_d$ radians/sec. Furthermore, we restrict the maximum allowed amplitudes of the audio and data signals individually in accordance with FCC regulations so that:

$$f_d \mid \mathrm{A}(t) \mid \leq 75\mathrm{kHz}; \quad \mathrm{f_d} \mid \mathrm{D(t)} \mid \leq 7.5\mathrm{kHz}. \quad (4)$$

The analog audio signal $A(t)$ is given by

$$A(t) = A_p\cos(\omega_p t) + V_{L+R}(t) + 2V_{L-R}(t)\cos(2\omega_p t). \quad (5)$$

The first term is the pilot signal of frequency $\omega_p = 2\pi f_p$, where $f_p = 19$ kHz; the second term $V_{L+R}(t)$ is the sum of left and right stereo signals; the third term is the difference of left and right stereo signals modulating a sinusoid of frequency $2f_p = 38$ kHz. The digital data signal modulates a subcarrier of frequency ω_{sc} and is given by

$$D(t) = c(t)\cos\omega_{sc}t \quad (6)$$

$$c(t) = \sum_{k=1}^{N} b_k g(t - kT), \quad (7)$$

where there are N bits of binary data b_k, sampled at intervals T seconds apart. In HSDS system [1] the shaping signal pulse $g(t)$ is the duobinary signal with $g(0) = g(T) = 1$, and $g(nT) = 0$, for $n \geq 2$. The subcarrier frequency $\omega_{sc}(= 2\pi f_{sc})$ is chosen so that the audio and data signals occupy disjoint parts of the baseband spectrum, and in our example $f_{sc} = 66.5$kHz. We assume that the audio signal $A(t)$ has Fourier components $A(f)$ such that it is confined to the spectral band $(0, f_A^+)$:

$$A(f) \neq 0 \Rightarrow 0 \leq f \leq f_A^+ \quad \mathrm{kHz}, \quad (8)$$

while the data signal $D(t)$ has Fourier components $D(f)$ such that it is confined to the spectral band (f_D^-, f_D^+)

$$D(f) \neq 0 \Rightarrow f_A^+ < f_D^- \leq f \leq f_D^+ \quad \mathrm{kHz}. \quad (9)$$

Specifically, we consider the case $f_A^+ = 53$kHz, $f_D^- = 57$kHz, and $f_D^+ = 76$kHz. In Figure 1, we show the

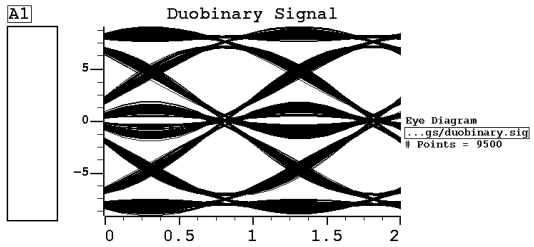

Figure 1: Eye diagram of the transmitted duobinary signal $c(t)$

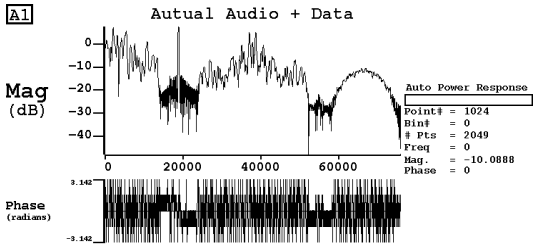

Figure 2: Power density spectrum of the multiplexed signal $S(t) = A(t) + D(t)$

eye diagram of the transmitted duobinary signal $c(t)$, and in Figure 2 we plot the power spectrum of the multiplexed signal $S(t) = A(t) + D(t)$. These were obtained from the SPW [5] simulator that we developed for the HSDS system.

3 Analysis of Multipath Interference

In Section 3.1 we derive the effect on the discriminator output of the interference from a discrete multipath channel consisting of a primary path plus M reflected paths. Our analysis is shown for both time varying and fixed multipath channels. In addition, the analysis is extended to a more general multipath channel, which does not necessarily consist of discrete multipath components. In Section 3.2 the power spectral density is derived under mild multipath conditions, while in Section 3.3 conditions under which the received signal displays almost linear behaviour are calculated for examples of two path and three path models, and the results are confirmed with simulations.

3.1 Multipath Interference Models

In the presence of multipath interference, the instantaneous frequency of the received signal is a nonlinear combination of the instantaneous frequency of the transmitted signal and its time delayed versions, as shown below. This nonlinearity of the frequency modulation produces complex interference effects. In the absence of multipath interference, the audio and data signals could be separated by filtering the instantaneous frequency in the baseband after demodulation, because the audio and data signals occupy separate frequency ranges, as specified by equations (8) and (9). However, when there is multipath interference, and thus nonlinearity of the instantaneous received frequency, the audio and data signals are no longer confined to separate parts of the baseband spectrum; hence, the multipath channel results in interference between the audio and data signals. The maximum amplitudes of $A(t)$ and $D(t)$ are regulated as in equation (4) so that typically the audio signal peak power is approximately 20 dB above the data signal. Thus it appears that multipath interference could potentially cause the audio signal to significantly degrade the data signal.

We express the transmitted frequency modulated signal as

$$X(t) = A\cos(\omega_c t + \theta_s(t)) \tag{10}$$

by letting

$$\theta_s(t) = \omega_d \int_0^t S(u)\,du = 2\pi f_d \int_0^t S(u)\,du \tag{11}$$

denote the phase of the FM signal.

In our earlier work [6] we discussed the simple two path model in some detail. Here we derive a general multipath model, but for simplicity, we illustrate this generalization for the case without additive noise. We consider a multipath model, in which the received signal consists of the primary path signal plus M additional reflected path signals:

$$\begin{aligned} Y(t) \;=\; & X(t) + \alpha_1 X(t-\tau_1,\theta_1) + \alpha_2 X(t-\tau_2,\theta_2) \\ & + \ldots + \alpha_M X(t-\tau_M,\theta_M), \end{aligned} \tag{12}$$

where the phase, attenuation, and delay of the i^{th} reflected path are denoted by θ_i, α_i, and τ_i respectively. By rewriting the received signal as

$$Y(t) = G(t)\cos(\omega_c t + \phi(t)), \tag{13}$$

the phase $\phi(t)$ term can be expressed as

$$\phi(t) = \theta_s(t) + \xi(t), \tag{14}$$

where $\theta_s(t)$ is the phase of the transmitted FM signal as defined in (11), and the difference $\xi(t)$ between the phases at the transmitter and the receiver is

$$\tan\xi(t) = \frac{\sum_{i=1}^{M}\alpha_i \sin(\psi_i(t))}{1+\sum_{i=1}^{M}\alpha_i\cos(\psi_i(t))}. \tag{15}$$

The function $\psi_i(t)$, which captures the effect of the i-th reflected signal on the distortion of the received signal, is given by

$$\begin{aligned} \psi_i(t) \;&=\; \theta_s(t-\tau_i) - \theta_s(t) - \omega_c\tau_i + \theta_i \\ &=\; \int_t^{t-\tau_i} [\omega_c + \omega_d S(u)]du + \theta_i. \end{aligned} \tag{16}$$

We consider time varying channel parameters $\alpha_i(t), \theta_i(t), \tau_i(t)$, as for a mobile user. The interference term in the FM discriminator output is then given by

$$\dot{\xi}(t) = \sum_{i=1}^{M}\Big(\eta_i(t)\dot{\psi}_i(t) + \rho_i(t)\dot{\alpha}_i(t)\Big), \tag{17}$$

where

$$\eta_i(t) = \frac{\alpha_i\cos\psi_i + \alpha_i\sum_{j=1}^{M}\alpha_j\cos(\psi_i-\psi_j)}{1+2\sum_{j=1}^{M}\alpha_j\cos\psi_j + \sum_{j=1}^{M}\sum_{k=1}^{M}\alpha_j\alpha_k\cos(\psi_j-\psi_k)} \tag{18}$$

$$\rho_i(t) = \frac{\sin\psi_i + \sum_{j=1}^{M}\alpha_j\sin(\psi_i-\psi_j)}{1+2\sum_{j=1}^{M}\alpha_j\cos\psi_j + \sum_{j=1}^{M}\sum_{k=1}^{M}\alpha_j\alpha_k\cos(\psi_j-\psi_k)} \tag{19}$$

$$\begin{aligned} \dot{\psi}_i(t) &= \dot{\theta}_s(t-\tau_i) - \dot{\theta}_s(t) - \omega_c\dot{\tau}_i(t) + \dot{\theta}_i(t) \\ &= 2\pi f_d[S(t-\tau_i) - S(t)] - \omega_c\dot{\tau}_i(t) + \dot{\theta}_i(t), \end{aligned} \tag{20}$$

when time variation of the carrier frequency is neglected and the inequality $\dot{\tau}_i(t) \ll 1$ is used. Equation (17) contains the contribution to the discriminator output from interference of the M reflected paths. The total discriminator output is given by

$$\begin{aligned} \dot{\phi}(t) \;=\; & 2\pi f_d\left[\left(1-\sum_{i=1}^{M}\eta_i(t)\right)S(t) + \sum_{i=1}^{M}\eta_i(t)S(t-\tau_i)\right] \\ & + \sum_{i=1}^{M}\eta_i(t)(-\omega_c\dot{\tau}_i(t) + \dot{\theta}_i(t)) + \sum_{i=1}^{M}\rho_i(t)\dot{\alpha}_i(t). \end{aligned} \tag{21}$$

Generally, the multipath parameter time derivatives satisfy $\mid \dot{\theta}_i(t) \mid \ll \mid \omega_c\dot{\tau}_i(t) \mid$, and $\dot{\tau}_i(t) \propto \frac{v}{c}$, where the user's velocity and the speed of light are given by v and c respectively.

When the contributions to the discriminator output from time variation of the channel can be neglected, the interference term of the discriminator output (equation (17)) reduces to

$$\dot{\xi}(t) = \sum_{i=1}^{M}\eta_i(t)\dot{\psi}_i(t), \tag{22}$$

where

$$\dot{\psi}_i(t) = \dot{\theta}_s(t-\tau_i) - \dot{\theta}_s(t) = 2\pi f_d[S(t-\tau_i) - S(t)], \tag{23}$$

and $\eta_i(t)$ is still given by (18). In this case, the total discriminator output becomes

$$\dot{\phi}(t) = 2\pi f_d\left[\left(1-\sum_{i=1}^{M}\eta_i(t)\right)S(t) + \sum_{i=1}^{M}\eta_i(t)S(t-\tau_i)\right]. \tag{24}$$

It is instructive to note that the output baseband signal resembles a weighted sum of the baseband signal $S(t)$ and its delayed replicas $S(t-\tau_i)$'s, for $i = 1, 2, \ldots, M$. The weights $\eta_i(t)$, however, can be negative and they depend on the signal S through the phases $\psi_i(t)$. Thus $\dot{\phi}(t)$ is in general a nonlinear combination of the transmitted signal and its time delayed versions. This output displays highly nonlinear behaviour under some conditions, while it displays almost linear behaviour under others, as shown in Section 3.3.

Since the discriminator output is equivalent to the instantaneous frequency, we can rewrite (24) as

$$\omega_r(t) = \left(1 - \sum_{i=1}^{M} \eta_i(t)\right) \omega(t) + \sum_{i=1}^{M} \eta_i(t)\omega(t-\tau_i) \quad (25)$$

where $\omega(t)$ and $\omega_r(t)$ are the instantaneous frequencies at the transmitter and the receiver, respectively.

The above analysis considered a channel consisting of $M+1$ discrete multipath components. We can consider a more general diffuse fading model so that equation (12) is generalized to:

$$Y(t) = \int d\tau \alpha_\tau(t) X(t-\tau, \theta_\tau(t)). \quad (26)$$

If the time variation of the channel parameters can be neglected, the interference term from the discriminator output becomes

$$\dot{\xi}(t) = \int d\tau \eta_\tau(t) \dot{\psi}_\tau(t), \quad (27)$$

where

$$\eta_\tau(t) = \frac{\alpha_\tau \int d\tau' \alpha_{\tau'} \cos(\psi_\tau(t) - \psi_{\tau'}(t))}{\int d\tau d\tau' \alpha_\tau \alpha_{\tau'} \cos(\psi_\tau(t) - \psi_{\tau'}(t))} \quad (28)$$

$$\dot{\psi}_\tau(t) = \dot{\theta}_s(t-\tau) - \dot{\theta}_s(t) = 2\pi f_d [S(t-\tau) - S(t)]. \quad (29)$$

It can be show that equations (26)–(29) reduce to equations (12), (22), (18), and (23) for the discrete channel model, where we use the notation $\theta_{\tau_i} = \theta_i, \psi_{\tau_i} = \psi_i$, and $\theta_0 = 0$.

3.2 Mild Multipath Conditions

We now calculate the power spectral density of the received signal in the digital frequency range (f_D^-, f_D^+) when the multipath interference is weak. In this section we consider a two path model, i.e., we set $M = 1$ in the discrete multipath model discussed above. We thus set $\alpha_1 = \alpha$ and $\tau_1 = \tau$.

Then Equation (25) simply reduces to

$$\omega_r(t) = (1 - \eta(t))\, \omega(t) + \eta(t)\omega(t-\tau) \quad (30)$$

where the weight $\eta(t)$ is given by

$$\eta(t) = \frac{\alpha\,(\alpha + \cos\psi_1(t))}{1 + 2\alpha\cos\psi_1(t) + \alpha^2}, \quad (31)$$

and has a time dependence from the phase

$$\psi_1(t) = \int_t^{t-\tau} \omega(u) du. \quad (32)$$

In the limit of small α and small τ we can obtain an analytic expression for the power spectral density. We derive this expression by first noting that for small α and small τ Taylor series approximations allow the received instantaneous frequency in the digital frequency range (f_D^-, f_D^+) to be written, after using trigonometric identities, as

$$\begin{aligned}
\omega_r(t) = & \int_{f_D^-}^{f_D^+} \left[Re\{D(f)\}\cos(2\pi f t) - Im\{D(f)\}\sin(2\pi f t)\right] df \\
& + 2\alpha\cos(2\pi f_c \tau) \int_{f_D^-}^{f_D^+} \sin(\pi f \tau) \\
& \quad \times \left[Re\{D(f)\}\sin(2\pi f(t - \frac{\tau}{2})) \right. \\
& \quad \left. + Im\{D(f)\}\cos(2\pi f(t - \frac{\tau}{2}))\right] df \\
& - 2\alpha\sin(2\pi f_c \tau) \int_0^{f_A^+} \int_0^{f_A^+} \sin(\pi f \tau)\sin(\pi f' \tau) \frac{1}{2\pi f'} \\
& \quad \times \left[Re\{A(f)\}Re\{A(f')\} - Im\{A(f)\}Im\{A(f')\}\right] \\
& \quad \times \sin\left(2\pi(f + f')(t - \frac{\tau}{2})\right) df\, df' + \ldots \quad (33)
\end{aligned}$$

Equation (33) includes terms up to order α. The first term in the equation is the transmitted digital data signal, while the remaining terms are due to multipath interference. The last term is due to the audio signal's interference in data frequency range $(f_D^-, f_D^+$ kHz). Although the transmitted audio signal is confined to the (0 - f_A^+ kHz) region, the nonlinearity in the received signal due to multipath, as seen in equation (30), produces these audio interference terms in $(f_D^-, f_D^+$ kHz). There are additional terms linear in α which depend on both $A(f)$ and $D(f)$.

We next compute the power spectral density $\Psi_r(f)$ of the received signal $\omega_r(t)$ in the data frequency range $f_D^- - f_D^+$ kHz, when both multipath parameters α and τ are small. We assume independent Gaussian random processes for the components $V_{L-R}(t)$ and $V_{L+R}(t)$ of the audio signal. Furthermore, we assume A(t) is independent of D(t). We denote

$$\Psi_D(f) = \text{power spectral density of D(t)} \quad (34)$$

$$\Psi_A(f) = \text{power spectral density of A(t)} \quad (35)$$

Using equation (33) and including additional terms to yield the power spectral density up to order α^2, we derive

$$\Psi_r(f) = \Psi_D(f)\left[1 - \frac{\alpha}{2}\cos(2\pi f_c \tau)\sin^2 \pi f \tau\right] \quad (36)$$

$$+ \alpha^2 \frac{\sin^2 2\pi f_c \tau}{16\pi^2} \int_0^{f_A^+} df_1 \Psi_A(f)\Psi_A(f-f_1) \times \sin^2(\pi f_1 \tau)\sin^2(\pi(f-f_1)\tau) \times \frac{1}{f_1}\left(\frac{1}{f_1}+\frac{1}{f-f_1}\right) + \ldots \quad (37)$$

The first term $\Psi_D(f)$ is the power spectral density of the transmitted data signal. The next term, the correction linear in α, is due to multipath interference of the data signal with itself. The remaining terms, which are quadratic in α, originate from the audio signal, which when the FM signal is passed through the multipath channel, contribute to the data frequency range $f_D^- - f_D^+$ kHz of the received demodulated signal. If values of $\tau \leq 1\mu$sec and $\alpha \leq .3$, along with $f_A^+ = 53$ kHz, are substituted into equation (36), then in the range $f_D^- = 57$ kHz to $f_D^+ = 76$ kHz for example, the multipath terms contribute only a small amount to the total power spectral density; hence, multipath effects are not significant here when the multipath parameters are small enough. For larger values of α and τ, interference effects can be investigated with SPW simulations.

3.3 Nonlinear Regions of Multipath Effects

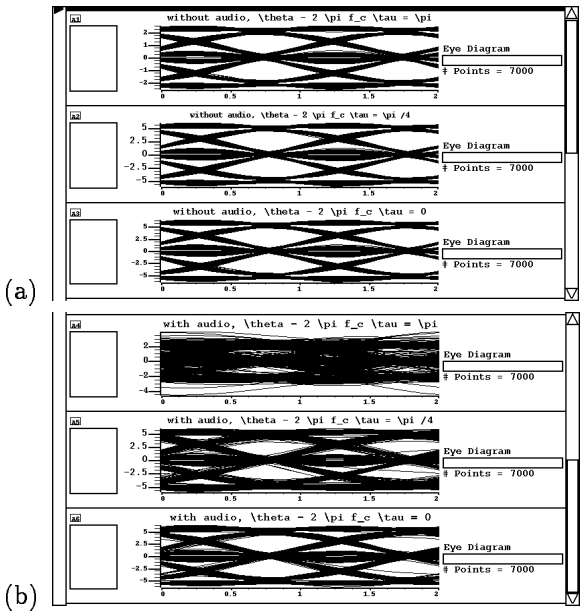

Figure 3: Two path model: $\alpha = .75, \tau = 2.06\mu$sec. (a) Eye diagram when only digital signal is transmitted. (b) Eye diagram when both audio and digital signals are transmitted.

The nonlinearities in the instantaneous frequency of the received signal $\omega_r(t)$ do not always occur, and it is useful to examine the circumstances under which they do and do not occur. In particular, it is these nonlinearities which result in audio signal interference with the received data signal. Certain combinations of f_c, f_d, and the multipath parameters result in linear behavior of $\omega_r(t)$, and hence eliminate the audio signal interference with the received data. We first describe how to find these linear regions for a discrete two path model and then for a discrete three path model. In each case, we compare our predicted linear regions with simulation results.

The instantaneous frequency $\omega_r(t)$ is given by equation (30) for a two path model, neglecting time variations of the channel parameters. It is seen that if $\eta(t)$ were constant, then $\omega_r(t)$ would be a simple linear combination of the instantaneous frequency of the transmitted signal and this same frequency delayed by τ in time. Equation (31) for $\eta(t)$ in the two path model is a function of $\cos\psi_1(t)$ for fixed α, and $\eta(t)$ is nearly constant for a sizable range of values of $\cos\psi_1(t)$ near 1. For example, for $\alpha = .75$, the value of $\eta(t)$ varies only from .36 to .43 for $0 \leq \cos\psi_1(t) \leq 1$. Thus $\eta(t)$ does not vary too much even within this large range, and hence $\omega_r(t)$ may not deviate too much from linearity even within this range. In order to find when $\cos\psi_1(t)$ lies in a particular range, we examine equation (32) to determine the range of $\psi_1(t)$. For example, the nearly linear region of $\eta(t)$ occurs for $\cos\psi_1(t)$ near 1, or equivalently when $\psi_1(t)$ lies near $n\pi$ with $n = 0, 2, 4, \ldots$.

Although the modulating signal $S(t)$ is unknown, the range of $\psi_1(t)$ can be determined. From equation (16), we see that $|\ \psi_1(t)\ |$ varies from

$$|\ \theta_i - \omega_c\tau + 2\pi \times 82.5\tau\ | \quad (38)$$

to

$$|\ \theta_i - \omega_c\tau - 2\pi \times 82.5\tau\ |, \quad (39)$$

because the FCC fixes the deviation frequency so that

$$f_d\ |\ S(u)\ | \leq 82.5\text{kHz}. \quad (40)$$

We can then determine the minimum and maximum values of $\cos\psi_1(t)$ from this range of $\psi_1(t)$. This range of values of $\cos\psi_1(t)$ in turn determines the range of $\eta(t)$ through (31). Therefore, the multipath attenuation α and time delay τ, as well as the phase $\theta_i - \omega_c\tau$, determine how closely $\omega_r(t)$ is to behaving linearly. In Table 1 we display the ranges of $\psi_1(t)$, $\cos\psi_1(t)$, and $\eta(t)$ for various values of $\theta_i - \omega_c\tau$, given multipath parameters of $\alpha = .75$ and $\tau = 2.06\mu$sec.

The smaller the range that $\eta(t)$ exhibits, or equivalently the more nearly constant $\eta(t)$ is, the more nearly linearly $\omega_r(t)$ behaves, according to equation (25). When $\omega_r(t)$ is linear, the audio signal will not

$\theta_1 - \omega_c\tau$	ψ_1(t)/2π	cos ψ_1(t)	η(t)
0	-.17 to .17	.48 to 1.00	.40 to .43
$\pi/4$	-.04 to .30	-.31 to 1.00	.30 to .43
π	.33 to .67	-1.00 to -.51	-3.00 to .23

Table 1: Ranges of ψ_1(t), cos $\psi_1(t)$, and η(t) in two path model for $\alpha = .75$ and $\tau = 2.06\mu$sec and various values of $\theta_1 - \omega_c\tau$.

interfere with the data, since the audio and data signals occupy disjoint parts of the baseband spectrum. As seen from the Table 1, when

$$\theta_i - \omega_c\tau = n\pi, \qquad n = 0, 2, 4, ... \tag{41}$$

there is very little variation in $\eta(t)$; hence, the behavior is almost linear, and thus we expect only a small amount of audio interference with the received data signal. Simulations of the HSDS system are shown in Figure 3a, which displays the eye diagram of the received data signal when no audio signal is transmitted, while Figure 3b displays the received data when an audio signal is also transmitted. Indeed, it is seen from Figure 3 that there is only a small amount of audio interference with the received data for $\theta_i - \omega_c\tau = 0$. Similarly, since $\theta_i - \omega_c\tau = \pi/4$ has a slightly greater range of $\eta(t)$ as seen from Table 1, but $\eta(t)$ is still not too far from being constant, we expect a little more interference of the audio signal with the received data. In Figure 3, the eye diagram of the received data when an audio signal is also transmitted is still pretty clear, and a little more interference from the audio signal is seen than for the case of $\theta_i - \omega_c\tau = 0$. Finally, for $\theta_i - \omega_c\tau = \pi$, the large range of $\eta(t)$ indicates much audio interference with the data signal, and indeed this is seen in Figure 3b.

We note that $-(\theta_i - \omega_c\tau)$ would produce the same degree of nonlinear behavior as $\theta_i - \omega_c\tau$, as seen from equations (38) and (39). Hence, almost linear behavior is seen for

$$-\pi/4 + n\pi \le \theta_i - \omega_c\tau \le \pi/4 + n\pi \qquad n = 0, 2, 4, ... \tag{42}$$

The range of ψ_1(t), obtained from the difference between equations (38) and (39), increases with τ and thus the range of $\theta_i - \omega_c\tau$ about 0 for which almost linear behavior and little audio interference is exhibited decreases with τ, and thus can be smaller than (42) for $\tau > 2.06\mu$sec, and larger for $\tau < 2.06\mu$sec.

As seen from the parameters used in Table 1, for a fixed multipath channel, as for a stationary user, the choice of the carrier frequency determines the degree of linearity. Alternatively, for a fixed carrier frequency, a mobile user will travel into and out of nonlinear regions, as the set of multipath parameters changes with the user's motion. If the effects of time varying channel parameters on the exact locations of nonlinear regions are required, equation (21) can be used instead of (24), which was used here.

We now show how to determine linear regions for the three path model. Using equation (25) for $M = 2$ reflected paths yields

$$\omega_r(t) = \Big(1-\eta_1(t)-\eta_2(t)\Big)\omega(t)+\eta_1(t)\omega(t-\tau_1)+\eta_2(t)\omega(t-\tau_2). \tag{43}$$

When $\eta_1(t)$ and $\eta_2(t)$ are relatively constant, the frequency of the received signal is approximately a linear combination of the frequency of the transmitted signal and its time delayed versions. When $M = 2$, equation (18) reduces to

$$\eta_1(t) = \eta(1, 2, t) \tag{44}$$

$$\eta_2(t) = \eta(2, 1, t), \tag{45}$$

where

$$\eta(i, k, t) = \frac{D}{N} \tag{46}$$

$$D = \alpha_i(\alpha_i + \cos\psi_i + \alpha_k\cos(\psi_i - \psi_k)) \tag{47}$$

$$N = 1 + \alpha_i^2 + \alpha_k^2 + 2\alpha_i\cos\psi_i + 2\alpha_k\cos\psi_k + 2\alpha_i\alpha_k\cos(\psi_i - \psi_k). \tag{48}$$

Since $\cos(\psi_i - \psi_k)$ can be expressed in terms of $\cos\psi_i$ and $\cos\psi_k$, the weights $\eta_1(t)$ and $\eta_2(t)$ are each functions of $\alpha_1, \alpha_2, \cos\psi_1$ and $\cos\psi_2$, where $\cos\psi_i$ in turn depends on τ_i and θ_i, for $i = 1, 2$. Thus for given $\alpha_1, \alpha_2, \tau_1, \tau_2$, we can determine the range of $\eta_1(t)$ and $\eta_2(t)$ for various values of the phases $\theta_i - \omega_c\tau_i$, as was done above for the two path example. Hence, for various values of $\theta_i - \omega_c\tau_i$ we compute the ranges of $\eta_1(t)$ and $\eta_2(t)$. The results are presented in Table 2, which is analogous to Table 1. We consider an example where $\alpha_1 = .75, \alpha_2 = .5, \tau_1 = 2.06\mu$sec, $\tau_2 = 3.29\mu$sec, and $\theta_1 - \omega_c\tau_1 = \theta_2 - \omega_c\tau_2$.

We compare the results to those from simulations using the same channel parameters. Eye diagrams from such simulations in which only a data signal is transmitted and in which both audio and data signals are transmitted are shown in Figures 4a and b respectively. From Table 2, it is seen that the ranges of $\eta_1(t)$ and $\eta_2(t)$ are not too large for $\theta_i - \omega_c\tau = 0$, and the corresponding eye diagram in Figure 4b is relatively open when the audio signal is transmitted with the data. As the phase $\theta_i - \omega_c\tau$ increases to $\pi/4$, the ranges of $\eta_1(t)$ and $\eta_2(t)$ become larger, and the corresponding eye diagram in Figure 4b closes more. Finally, when $\theta_i - \omega_c\tau = \pi$, the ranges of $\eta_1(t)$ and $\eta_2(t)$ are quite large, and the corresponding eye diagram is closed. Hence, for the three path model, almost linear behaviour is exhibited for

$$\theta_i - \omega_c\tau_i \approx n\pi. \qquad n = 0, 2, 4, ... \tag{49}$$

$\theta_i - \omega_c \tau_i$	$\psi_1(t)/2\pi$	$\cos\psi_1(t)$	$\psi_2(t)/2\pi$	$\cos\psi_2(t)$	$\eta_1(t)$	$\eta_2(t)$
0	-.17 to .17	.48 to 1.00	-.27 to .27	-.13 to 1.00	.28 to .41	.04 to .25
$\pi/4$	-.04 to .30	-.31 to 1.00	-.14 to .39	-.77 to 1.00	.10 to .53	-.22 to .32
π	.33 to .67	-1.00 to -.51	.23 to .77	-1.00 to .13	-.68 to 2.97	-.14 to 1.97

Table 2: Ranges of $\psi_i(t)$, $\cos\psi_i(t)$, and $\eta_i(t)$ in three path model for $\alpha_1 = .75, \alpha_2 = .5, \tau_1 = 2.06\mu$sec, $\tau_2 = 3.29\mu$sec and various values of $\theta_i - \omega_c \tau_i$.

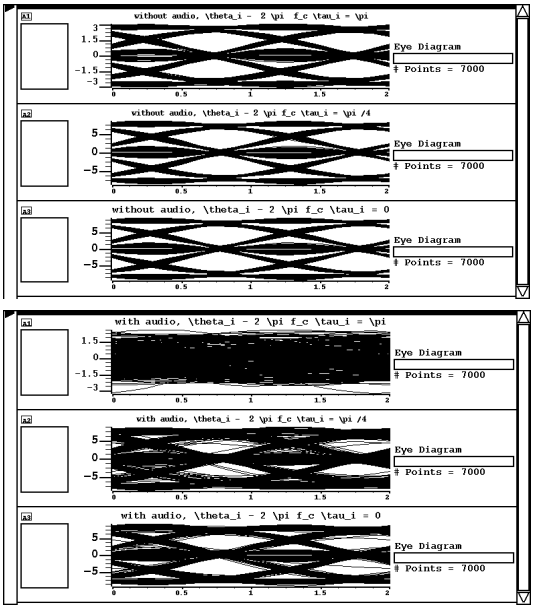

Figure 4: Three path model: $\alpha_1 = .75, \tau_1 = 2.06\mu$sec, $\alpha_2 = .5, \tau_2 = 3.29\mu$sec (a) Eye diagram when only digital signal is transmitted. (b) Eye diagram when both audio and digital signals are transmitted.

We have used our analytical results derived in Section 3.1 to calculate ranges in which the received signal should behave almost linearly for examples of two path and three path models. Simulation results agree with these calculations, showing little audio interference in the calculated almost linear regions and significant audio interference outside these regions.

4 Concluding Remarks

We have developed analytical techniques to study the adverse effects of multipath interference on an FM subcarrier data signal. Considering a general multipath interference model that can be used to represent many types of channels, we have obtained a closed form expression for the signal received from a discriminator. We have described the nonlinear interference that will develop between the audio signal $A(t)$ and digital signal $D(t)$. Using this analsyis, we have calculated and confirmed with simulations, by constructing a fairly comprehensive SPW simulator of a representative system (i.e., HSDS system), the conditions under which this interference is almost linear.

Further simulations can illustrate all the effects we have presented in our analysis here: such simulations should include the effects of additive WGN and time varying channel parameters, as well as use of more than three multipath components. These effects have been incorporated into our analysis as seen above.

The multipath interference analysis we have developed may prove useful when applied to noncoherent reception of GSM, which uses GMSK (Gaussian-filtered minimum shift keying), as well as to noncoherent detection in other wireless systems.

Acknowledgments:
The present work has been supported, in part, by the National Science Foundation, New Jersey Commission on Science and Technology, Seiko Communications, and the Ogasawara Foundation for the Promotion of Science and Engineering.

References

[1] G. Gaskill and K. Gray, "Seiko High Speed Subcarrier Data System, (HSDS) White paper," Seiko Telecommunication Systems, Inc., Beaverton, Oregon, September 21, 1993.

[2] Kuroda, T., M. Takada, T. Isobe, and O. Yamada, "Transmission Scheme of High Capacity FM Multiplex Broadcasting System," *IEEE Trans. Broadcasting*, Vol. 42, No. 3, pp. 245-250, Sept. 1996.

[3] J-P. M. G. Linnartz, "Spectrum Efficiency of Radio Data System (RDS)," *IEEE Trans. Broadcasting,* Vol. 39, No. 3, September 1993, pp. 331-334.

[4] Schwartz, M., W. R. Bennet, and S, Stein, *Communication Systems, and Techniques*, McGraw-Hill, Inc., 1966.

[5] *Signal Processing WorkSystem*, Alta Group of Cadence Design Systems, Inc., 1996.

[6] Zeger, L., P. Chen and H. Kobayashi, "Effects of Multipath Interference on an FM Data Subcarrier". *Proc. of the 1997 IEEE Pacific Rim Conference on Communications, Computers and Signal Processing (PACRIM'97)*, pp. 40-44, Victoria, B.C., Canada, August 20-22, 1997.